INDERSCIENCE PUBLISHERS
Linking academia, business and industry through research


**International Journal of Advanced Mechatronic Systems**

ISSN online: 1756-8420 - ISSN print: 1756-8412
https://www.inderscience.com/ijamechs

# Swing-up design of double inverted pendulum by using passive control method based on operator theory

Ni Bu, Xiaoguang Wang

**DOI:** 10.1504/IJAMECHS.2022.10047303

**Article History:**

| | |
|---|---|
| Received: | 13 January 2022 |
| Accepted: | 14 March 2022 |
| Published online: | 09 January 2023 |

*Copyright © 2023 Inderscience Enterprises Ltd.*

# Swing-up design of double inverted pendulum by using passive control method based on operator theory

Ni Bu* and Xiaoguang Wang

College of Automation and Electronic Engineering,
Qingdao University of Science and Technology,
Qingdao 266061, China
Email: bunihan@163.com
Email: w18660479414@163.com
*Corresponding author

**Abstract:** For the double inverted pendulum system with limited guide rails, a self-starting pendulum control scheme by combining the passivity-based control (PBC) and operator-based robust right coprime factorisation (ORRCF) method is proposed. A three-step hierarchical swing control scheme is designed, and the control method of each step and the switching rules between each step are given. The passivity and robustness of the system are improved by the control scheme of PBC combined with ORRCF method, and the entire self-lifting and stabilisation process is controlled. The influence of external disturbance during the switching process of the swing control and the state change of the pendulum rod on the displacement of the car is overcome. The effectiveness of the control scheme has been verified by the simulation results.

**Keywords:** passivity-based control; robust right coprime factorisation; operator theory; double inverted pendulum; swing-up control.

**Reference** to this paper should be made as follows: Bu, N. and Wang, X. (2023) 'Swing-up design of double inverted pendulum by using passive control method based on operator theory', *Int. J. Advanced Mechatronic Systems*, Vol. 10, No. 1, pp.1–7.

**Biographical notes:** Ni Bu holds a PhD. She is an Associate Professor. Her main research directions are soft robot system design, nonlinear system control and design, optimal control, sliding mode control, etc.

Xiaoguang Wang is a master's student. Her main research direction is robust control of nonlinear systems.

## 1 Introduction

As a typical unstable nonlinear system, the inverted pendulum is the simplest model for many control objects (Liu et al., 2021; Bi et al., 2015). Its research mainly involves two aspects: steady swing control and start swing control. Commonly used slew control methods include LQR method (Zhou, 2020), improved PID parameter method (He et al., 2021), and adaptive fault-tolerant fuzzy control method (Henmi et al., 2003). Commonly used swing control includes energy control (Henmi et al., 2005), genetic algorithm control (Henmi et al., 2014) and sliding mode predictive variable structure control (Deng et al., 2006). The annular inverted pendulum system in the above literature does not have the problem of limited guide rails. However, the control of the linear inverted pendulum system will reduce the success rate of the start-up of the inverted pendulum due to the limited guide rails. Furthermore, the limitations of above control strategies lead to insufficient robustness and adaptability of the system after oscillation stabilisation.

The inverted pendulum is a complex nonlinear system with multiple degrees of freedom, and its swing-up input is considered as a disturbance. Thus, the requirements for achieving stable pendulum are more stringent. Compared with the energy control method based on Lyapunov function (Henmi et al., 2010), passive energy control has more practical significance in engineering design. The core idea of the passivity theory is to control the target physical quantity by controlling the energy (Bu and Deng, 2016; Deng and Bu, 2012, 2016). The ORRCF method has strong robustness to nonlinear systems with perturbation, including the following three advantages (Bu et al., 2020, 2021; Chen and Qian, 2021; Takasu et al., 2020; Deng et al., 2009, 2011):

1. Only the input-output model is used, avoiding the measurement of the real system state.
2. The extended Banach space is more suitable for system control theory and engineering.
3. The robust stability of nonlinear systems can be achieved by a Bezout identity and a norm inequalities.

Copyright © 2023 Inderscience Enterprises Ltd.

Based on the problems existing in the above research, a self-swing control scheme combining ORRCF method and PBC is proposed. The purpose of controlling the displacement of the car and the angle of the pendulum rod is realised through energy control. The control scheme consists of three steps. The first step is to design the switching control law based on the Lyapunov direct method. Swing the first-stage pendulum into a vertical inverted position while coordinating the swings of the two pendulums. In the second step, the PBC method based on operator theory ensures that the first-stage pendulum is stable in the inverted position. Then we use the quasi-car method to swing the second-stage pendulum rod and combine the energy control to make it smoothly enter the inverted position. In the third step, the control scheme of combining ORRCF method and PBC is used to stabilise the two pendulums in the inverted position at the same time. The scheme can overcome the influence of external perturbation during the switching process and weaken the influence of the pendulum swing amplitude change on the displacement of the car. Finally, the passiveness and robustness of the system are guaranteed, and the swing and stable control of the double inverted pendulum is realised.

## 2 Preliminaries

### 2.1 Robust right coprime factorisation

The definition of the operator is on the linear space of the extended Banach space, which is more suitable for practical applications than the general linear space. Moreover, it has a wide range of applications. It is not affected by linearity or nonlinearity, and is not limited by dimensionality. Robust right coprime factorisation can quickly ensure the robust stability of the system when dealing with systems with uncertainty.

*Definition 1:* The operator $P$: $U \to Y$ is a stable nonlinear operator with a right factorisation denoted as $P = ND^{-1}$. If there are two stable operator $A$: $Y \to U$ and $B$: $U \to U$, where $B$ is reversible. The unimodular operator $M \in (W, U)$, satisfies the Bezout identity:

$$AN + BD = M \tag{1}$$

Thus, the operator $P$ in the system shown in Figure 1 has a right coprime factorisation over the domain of definition, wherein $W$ is called a quasi-state space. Since the Bezout identity is satisfied for the operator $A$, $N$, $B$, $D$, the nonlinear feedback system in Figure 1 can be equivalent to Figure 2.

**Figure 1** Nonlinear feedback control system

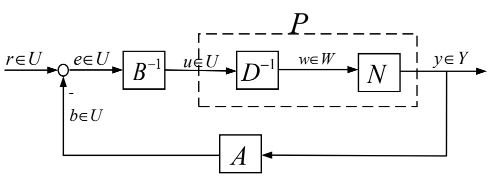


**Figure 2** Equivalent diagram of Figure 1

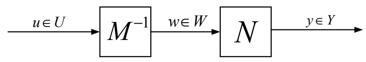


### 2.2 Passivity-based operator theory

Passive control is an inherently stable nonlinear control method, which can achieve global stability of the system. The nonlinear system $\Omega$ described in this paper by the operator form is expressed as follows:

$$\Omega : \begin{cases} \omega(t) = D^{-1}(u)(t) \\ y(t) = N(\omega)(t) \end{cases} \tag{2}$$

where $u \in U$, $\omega \in W$, $y \in Y$ are the control input, quasi-state and system output, respectively.

*Definition 2 (Deng and Bu, 2012):* If the nonlinear system $\Omega$ is a passive system, there exists a non-negative function $V : W \to R_+$ ($R_+$ is any non-negative real number), called a stored function, which satisfies the following conditions:

$$V(\omega) - V(\omega_0) \leq \int_0^t y(s)u(s)ds \tag{3}$$

where $\forall u \in U$, $\omega_0 \in W$, $t \geq 0$, and $y(s)u(s)$ is called the supply energy function.

If the non-negative function $V$ is differential, then the passive inequality (3) is equivalent to

$$\dot{V}(\omega) \leq y(t)u(t) \tag{4}$$

## 3 Inverted pendulum model

This part adopts the Lagrange method for modelling. The physical model of the double inverted pendulum is shown in Figure 3, and the specific physical parameters are shown in Table 1. In addition, $F_N(N)$ is the external force acting on the system, $x(m)$ is the displacement of the car, and $\theta_1(rad)$, $\theta_2(rad)$ is the angle of the pendulum rod. The existing literature (Zhang et al., 2011) ignores the influence of the mass $m_3$ at the link point between the cascade pendulum rods during modelling. However, this effect needs to be considered in the actual system. Therefore, this paper takes it into account in the system modelling analysis, making it more in line with the actual control of the inverted pendulum system.

**Table 1** Physical parameters

| *Parameter name* | *Parameter* | *Value* |
|---|---|---|
| The weight of the car | $m_0$ | 1.32 kg |
| The mass of swing rod 1 | $m_1$ | 0.04 kg |
| Rotation radius of swing rod 1 | $l_1$ | 0.0775 m |
| The mass of swing rod 2 | $m_2$ | 0.132 kg |
| Rotation radius of swing rod 2 | $l_2$ | 0.25 m |
| The mass of the mass block | $m_3$ | 0.208 kg |

**Figure 3** Physical model of double inverted pendulum

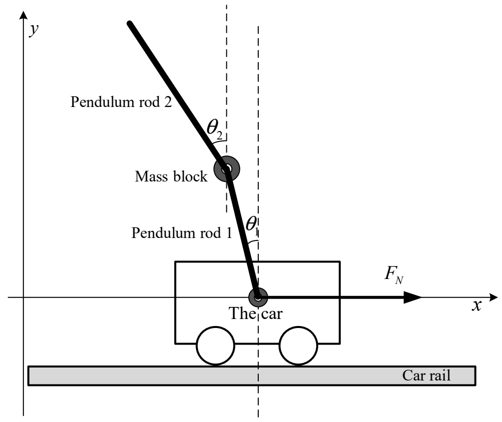


The total kinetic energy and total potential energy of the double inverted pendulum are expressed as follows:

$$\begin{aligned}T &= T_{m0} + T_{m1} + T_{m2} + T_{m3} \\ &= \frac{1}{2}m_0\dot{x}^2 + \frac{1}{2}m_1\dot{x}^2 - m_1 l_1 \dot{x}\dot{\theta}_1 \cos\theta_1 + \frac{2}{3}m_1 l_1 \dot{\theta}_1^2 \\ &+ \frac{1}{2}m_2\left(\dot{x}^2 - 2\dot{x}\left(2l_1\dot{\theta}_1 + l_2\dot{\theta}_2\cos\theta_2\right)\right) \\ &+ \frac{1}{2}m_2\left(4l_1^2\dot{\theta}_1^2 + \frac{4}{3}l_2^2\dot{\theta}_2^2 + 4l_1 l_2\dot{\theta}_1\dot{\theta}_2\cos(\theta_2 - \theta_1)\right) \\ &+ \frac{1}{2}m_3\dot{x}^2 - 2m_3 l_1\dot{x}\dot{\theta}_1\cos\theta_1 + 2m_3 l_1^2\dot{\theta}_1^2\end{aligned} \tag{5}$$

$$\begin{aligned}V &= V_{m0} + V_{m1} + V_{m2} + V_{m3} \\ &= 0 + m_1 g l_1 \cos\theta_1 + 2m_3 g l_1 \cos\theta_1 \\ &+ m_2 g\left(2l_1\cos\theta_1 + l_2\cos\theta_2\right)\end{aligned} \tag{6}$$

Equations (5)–(6) are modelled by the Lagrangian method, and the dynamic equation of the double inverted pendulum is obtained.

$$\begin{aligned}&-\left(m_1 l_1 + 2m_2 l_1 + 2m_3 l_1\right)\left(\ddot{x}\cos\theta_1 + g\sin\theta_1\right) \\ &+\left(\frac{4}{3}m_1 + 4m_2 + 4m_3\right)l_1^2\ddot{\theta}_1 + 2m_2 l_1 l_2\ddot{\theta}_2\cos(\theta_2 - \theta_1) \\ &-2m_2 l_1 l_2\dot{\theta}_2^2\sin(\theta_2 - \theta_1) = 0\end{aligned} \tag{7}$$

$$\begin{aligned}&-m_2 l_2\left(\ddot{x}\cos\theta_2 + g\sin\theta_2\right) + \frac{4}{3}m_2 l_2^2\ddot{\theta}_2 \\ &+2m_2 l_1 l_2\left\{\dot{\theta}_1^2\sin(\theta_1 - \theta_2) + \ddot{\theta}_1\cos(\theta_2 - \theta_1)\right\} = 0\end{aligned} \tag{8}$$

Meanwhile, the acceleration control method is adopted

$$u = \ddot{x} \tag{9}$$

## 4 Switch control scheme

The swing control of the double inverted pendulum is accomplished by swinging the pendulum rods one by one. Assume that the clockwise direction of the pendulum swing is positive, that is, the angular velocity $\dot{\theta}_i > 0\ (i = 1, 2)$. The control scheme is divided into three steps. Based on the state of the system, the control scheme of each step and the switching rules between each step are given.

### *4.1 The swing of the first-stage pendulum*

This part is mainly to swing the first-stage pendulum to near the inverted position, while coordinating the pacing of the two pendulums. For the swing-up control, the switching control law $u_1$ is designed using the energy control method of the Lyapunov function. The kinetic equation degenerated from the double inverted pendulum models (7)–(9) to a first-stage inverted pendulum is expressed as:

$$\begin{cases}\left(m_1 l_1 + 2m_3 l_1\right)\left(\ddot{x}\cos\theta_1 + g\sin\theta_1\right) \\ \quad = \left(\dfrac{4}{3}m_1 + 4m_3\right)l_1^2\ddot{\theta}_1 \\ u = \ddot{x}\end{cases} \tag{10}$$

First of all, the energy of the first-stage pendulum rod is expressed as follows:

$$E_1 = \frac{1}{2}\left(\frac{4}{3}m_1 + 4m_3\right)\dot{\theta}_1^2 + \left(m_1 g l_1 + 2m_3 g l_1\right)\left(\cos\theta_1 - 1\right) \tag{11}$$

where it is agreed that the inverted position of the first-stage pendulum rod is zero potential energy point.

When the pendulum is in an unstable equilibrium position, i.e., $\theta_1 = 0$ and $\dot{\theta}_1 = 0$, then $E_1 = 0$. When the pendulum is in a natural equilibrium position, i.e., $\theta_1 = \pi$ and $\dot{\theta}_1 = 0$, then $E_1 = -2m_1 g l_1$. Compute the derivative of $E_1$:

$$\dot{E}_1 \triangleq \frac{dE_1}{dt} = -\left(m_1 + 2m_3\right)l_1 u\dot{\theta}_1\cos\theta_1 \tag{12}$$

Define function $V_1 \triangleq 1/2E_1^2$. Then using Lyapunov's direct method and compute its differential:

$$\dot{V}_1 = -E_1\left(m_1 + 2m_3\right)l_1 u\dot{\theta}_1\cos\theta_1 \tag{13}$$

In order to ensure $\dot{V}_1 \leq 0$, $u_1$ can be designed according to the following rules. The design control input is expressed as follows:

$$u_1 \triangleq u = \lambda_1 \operatorname{sign}\left(E_1\dot{\theta}_1\cos\theta_1\right) \tag{14}$$

where $\lambda_1 > 0$ is the parameter that needs to be designed. The switching method includes two situations:

1. when the swing angle is $\theta_1 \in (\pi/2, \pi)$ or $\theta_1 \in (-\pi, -\pi/2)$ and the pendulum swings clockwise, the control input is $-\lambda_1$; when it swings counter-clockwise, it is switched to $\lambda_1$
2. when the swing angle is $\theta_1 \in (0, \pi/2)$ or $\theta_1 \in (-\pi/2, 0)$ and the pendulum swings clockwise, the control input is $\lambda_1$; When it swings counter-clockwise, it switches to $-\lambda_1$.

Due to the strong coupling between the two pendulums, the energy of the first-stage inverted pendulum is always lost due to the viscous friction during the swinging of the pendulum. The effect of the second pendulum on the first pendulum can be in two ways. It may cause it to lose energy, or it may accumulate energy. Therefore, we assume that the motion poses of the two pendulums can be coordinated by changing the input gain.

## 4.2 Swing the second-stage pendulum while stabilising the first-stage pendulum

The control scheme given in the second step is to make the second pendulum swing upward on the basis of ensuring the stability of the first pendulum. The proposed control method consists of two control laws $u = u_{21} + u_{22}$. The control scheme combining ORRCF method and PBC is used to ensure that the first-stage pendulum is stable at the unstable equilibrium point. The control law of this part is denoted by $u_{21}$. The model analysis is carried out by the quasi-car method, and the second-stage pendulum is swung up to the inverted position in combination with the energy control method. The control law of this part is denoted by $u_{22}$.

### 4.2.1 Steady control of first-stage inverted pendulum

The system model is obtained from the first-stage inverted pendulum dynamic equation (10):

$$u_{\theta_1} = c\frac{\ddot{\theta}_1}{\cos\theta_1} - g\tan\theta_1 \tag{15}$$

where $\theta_1 \neq \pm\pi/2$ (i.e., the pendulum is not controllable when the pendulum is in a horizontal position), $c = 0.15$, and the gravitational acceleration is $g = 9.8$ m/s$^2$.

Figure 1 shows the right coprime factorisation of the research object of the nonlinear system, and Figure 2 is its equivalent figure. The corresponding symbol of the first-stage inverted pendulum control system is represented by $\{P_1, N_1, D_1, M_1, A_1, B_1, e_1\}$. First, the ORRCF method is used to factorise the operator model of the system:

$$P_1^{-1} = D_1 N_1^{-1} : y_1(\theta_1) \rightarrow x_1(\tilde{u}_{\theta_1}) \tag{16}$$

Based on the idea of isomorphism (Bu and Deng, 2011), the factorisation of the mathematical model of the first-stage inverted pendulum system is realised. Operators $N_1$ and $D_1$ can be represented as follows:

$$\begin{aligned} &N_1(\theta_1)(t) = I(\theta_1)(t) = \theta_1(t) \\ &D_1(\theta_1)(t) = c\frac{\ddot{\theta}_1(t)}{\cos\theta_1(t)} - g\tan\theta_1(t) \end{aligned} \tag{17}$$

Then, the PBC method is adopted to ensure the passiveness of the inverted pendulum system. Storage function $V_{P1}(\omega)(t)$ is designed as follows:

$$V_{P1}(\omega)(t) = \int_0^t M_1 D_1(\omega)(s)ds, \ |M_1(\omega)(t)| \leq |N_1(\omega)(t)| \tag{18}$$

The differential $\dot{V}_{P1}(\omega)(t)$ representation of the stored function is as follows:

$$\dot{V}_{P1}(\omega)(t) = M_1 D_1(\omega)(t), \ |M_1(\omega)(t)| \leq |N_1(\omega)(t)| \tag{19}$$

According to the properties of the operator, the Bezout identity $A_1N_1 + B_1D_1 = M_1$ needs to be satisfied. The designed stable controllers $A_1$ and $B_1$ are expressed as follows:

$$\begin{aligned} &A_1(\theta_1)(t) = \alpha_1\theta_1(t) - \frac{1}{\beta_1}\left(c\frac{\ddot{\theta}_1(t)}{\cos\theta_1(t)} - g\tan\theta_1(t)\right) \\ &B_1(u_{\theta_1})(t) = \frac{1}{\beta_1}u_{\theta_1}(t) \end{aligned} \tag{20}$$

where $0 < \alpha_1 \leq 1$, $\beta_1 > 0$ are the parameters to be designed.

Then, $M_1 = A_1N_1 + B_1D_1 = \alpha_1\theta_1(t) = \alpha_1 I(\theta_1(t))$ can be obtained from equations (17) and (20). It can be seen that $M_1$ is a unimodular operator, which can ensure the stability of the nonlinear feedback system. Meanwhile, it also satisfies the passive condition:

$$\dot{V}_{P1}(\omega)(t) \leq y_1(t)u_{\theta_1}(t) \tag{21}$$

where $y_1(t)u_{\theta_1}(t) = N_1(\omega)(t)D_1(\omega)(t)$. Then it also shows that the designed controller guarantees the passivity of the system with storage function.

Therefore, the control scheme guarantees the stability and passivity of the inverted pendulum system. According to the right factorisation principle shown in Figure 1, the control switching law of the first-stage inverted pendulum can be designed as:

$$u_{21} = B_1^{-1}\text{sign}(e_1) = \beta_1\text{sign}(e_1) \tag{22}$$

where $e_1(|e_1| \leq \delta)$ is the error of convergence to the desired angle in the first-stage inverted pendulum control.

### 4.2.2 Swing the second-stage pendulum by using the quasi-car method

Firstly, the quasi-car method is used to analyse the model of the second-stage inverted pendulum. Then, the second-stage pendulum rod is swung up by the same method as the first step, and the control law $u_{22}$ of the swing is designed.

**Figure 4** Geometric description of the quasi-car swing-up principle

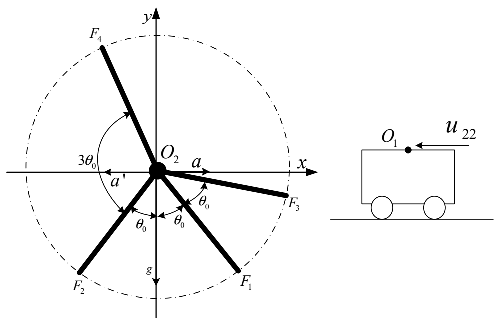


As shown in Figure 4, the concept of 'quasi-car' is introduced, that is, the car, the first-stage pendulum and the mass at the pivot are regarded as a whole. In this way, the acceleration $a$ on the link point $O_2$ can be regarded as being directly exerted on it by the 'quasi-car'. In addition, $O_1$ represents the link point of the first-stage pendulum rod and the car, $O_2$ represents the link point of the first-stage and second-stage pendulum rods, $O_2F_1$ represents the swing position of the second-stage pendulum rod, $a$ represents the external force acceleration at $O_2$, and the friction between the pendulum rod and the connection with the car is ignored.

Suppose there are three swing strategies (Åström and Furuta, 2000):

1 The second-stage pendulum swings from $O_2F_1$. Under the influence of gravitational acceleration $g$ and external force acceleration $a$ ($a > 0$), the second-stage pendulum will swing to $O_2F_2$ with the y-axis as the symmetry axis. Its swing angle is $2\theta_0$.

2 When the pendulum is in the $O_2F_2$ position, the pendulum rod changes the swing direction, that is, the direction of the acceleration is reversed to $a'$ ($a' = -a$). Under the combined action of this acceleration and the acceleration of gravity $g$, the pendulum swings to $O_2F_3$. Its swing angle is $3\theta_0$.

3 Then the pendulum rod reverses the direction again and swings to the $O_2F_4$ position with $O_2F_2$ as the axis of symmetry. Its swing angle is $6\theta_0$. At this point, the pendulum rod reaches near the unstable equilibrium point.

The above swinging process is repeated until the second-stage swing bar obtains the required energy, so that the two swing angles gradually converge to the inverted position.

The $a$ shown in Figure 4 is equal to the acceleration $u_{22}$ applied by the car on the link point $O_1$ but in the opposite direction. Assume that the clockwise rotation angle and the acceleration to the right are positive. The following control law is designed:

$$u_{22} = -a = -\beta_{21} sign(\dot{\theta}_2), \quad |\theta_2| > \sigma \tag{23}$$

where $\sigma > 0$, $\beta_{21} > 0$, are parameters that need to be designed.

In the case where the second-stage pendulum swings to a certain angle (i.e., $\varepsilon_2 \le \theta_2 \le \sigma$), $u_{22}$ is designed by using the energy method similar to the first step. The specific design method is shown in Section 3.1. From the principle of the quasi-car method and formula (14), we can get

$$u_{22} = -a = -\beta_{22}\mathrm{sign}\left(E_2\dot{\theta}_2 \cos\theta_2\right), \quad |\theta_2| \le \sigma \tag{24}$$

where $\beta_{22} > 0$ is the parameter to be designed.

### *4.3 Stability control of double inverted pendulum*

When the second-stage pendulum rod swings to the vicinity of the vertical inverted position, the control law is switched to the swing control law of the second-stage pendulum rod. At this stage, the control scheme of combining the ORRCF method and PBC described above is still adopted. The corresponding symbol for the control of the secondary inverted pendulum system is denoted by $\{P_i, N_i, D_i, M_i, A_i, B_i, e_{3i}\}$. The Taylor series of equations (7)–(9) around the equilibrium point are expanded and linearised. Then, by substituting the parameters in Table 1, the mathematical model of the double inverted pendulum system can be further simplified:

$$\ddot{\boldsymbol{\theta}} = H\boldsymbol{\theta} + Gu \triangleq H\boldsymbol{\theta} + \boldsymbol{u_\theta}$$

where $\boldsymbol{u_\theta} = [6.64\ -0.088]^T u$, $\boldsymbol{\theta}(t) = [\theta_1(t)\ \ \theta_2(t)]^T$, and $H$, $G$ are coefficient matrices.

The specific design method is shown in Section 3.2.1 of this paper. The control law of the secondary inverted pendulum is designed according to formula (22):

$$u_3 = B_i^{-1} sign(e_{3i}) = \beta_{3i} sign(e_{3i}) \tag{26}$$

where $\beta_{3i} = [\beta_{31}\ \beta_{32}]^T$ is the parameters to be designed. $|e_{3i}| \le \delta$ ($i = 1, 2$) is the error that the pendulum rod 1 and the pendulum rod 2 converging to the desired angle in the swing control.

In summary, the overall control scheme of the secondary inverted pendulum system is summarised as follows:

$$u = \begin{cases} u_1 = \lambda_1 sign\left(E_1\dot{\theta}_1 \cos\theta_1\right), & |\theta_1| > \varepsilon_1 \\ u_2 = u_{21} + u_{22}, & |\theta_1| \le \varepsilon_1, |\theta_2| > \varepsilon_2 \\ \begin{cases} u_{21} = \beta_1 sign(e_1), & \\ u_{22} = \begin{cases} -\beta_{21} sign(\dot{\theta}_2), & |\theta_2| > \sigma \\ -\beta_{22} sign\left(E_2\dot{\theta}_2 \cos\theta_2\right), & |\theta_2| \le \sigma \end{cases} \end{cases} & \\ u_3 = \beta_{3i} sign(e_{3i}), & |\theta_1| \le \varepsilon_1, |\theta_2| \le \varepsilon_2 \end{cases} \tag{27}$$

## 5 Simulation results

In order to verify the effectiveness of the control scheme in this paper, the parameters are selected as follows: $\alpha_1 = 1/3$, $\beta_1 = 1/6$, $\alpha_{3i} = [1/3\ 1/3]^T$, $\beta_{3i} = [1/6\ 1/6]^T$, $\varepsilon_1 = 0.19$ (rad), $\varepsilon_2 = 0.113$ (rad), $\sigma = 1.049$ (rad), and simulation experiments are carried out corresponding to the above parameters. According to formula (27), we have plotted the response curve of the control input signal as shown in Figure 5. Figures 6 and 7 are the simulation curve of the double inverted pendulum automatic swing control. The results show that the control scheme in this paper can successfully realise the self-swing control and swing the two pendulum rods to the inverted position in a short time.

First of all, under the action of control input $u_1$, the pendulum rod 1 starts to swing from the vertical downward position (i.e., $\theta_1 = \pi$), and swings to near the inverted position at 6s. Then switch to control input $u_2$. Under the action of the control input $u_{21}$, the oscillation of the swing angle $\theta_1$ converges around zero (i.e., $|\theta_1| \le \varepsilon_1$). At the same time, the pendulum rod 2 is swing up to achieve the purpose of coordinating the pace between the two pendulum rods:

1 when $|\theta_2| > \sigma$, the $u_{22}$ designed by the quasi-car method gathers energy for the second-stage pendulum rod to achieve the desired height of the swing

2 when $|\theta_2| \le \sigma$, the $u_{22}$ designed by the energy method can avoid energy dissipation and lead to control failure.

Notice: if $u_{22}$ is too large, the buffeting of the system will be serious, then the first pendulum will not be able to stabilise in the vertical position; if $u_{22}$ is too small, the system will not be able to provide enough energy for the second pendulum. Therefore, the value of $u_{22}$ cannot be too large or too small, so that the pendulum rod 1 can be vertically inverted and the pendulum rod 2 can be smoothly swung up. That is to say, the value of $u_{22}$ limits the displacement of the car to a certain extent, which also satisfies the condition that the guide rail is limited. In the end, when the angle of pendulum 2 is within a certain range (i.e., $\varepsilon_2 \le \theta_2 \le \sigma$), it switches to the control input $u_3$, at which time $\theta_2$ gradually oscillates and converges to near zero.

**Figure 5** Control input signal *u* (see online version for colours)

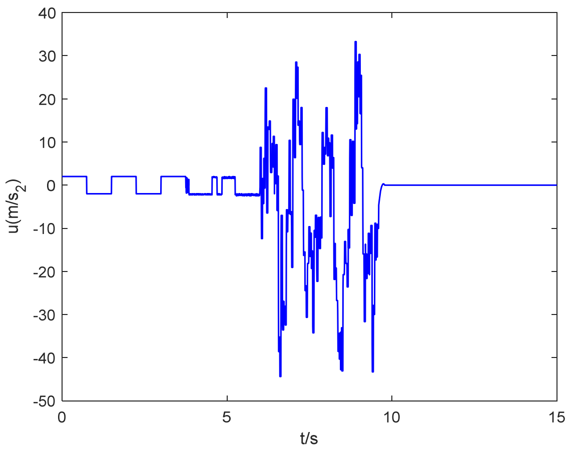


**Figure 6** Response curve of pendulum 1 angle $\theta_1$ (see online version for colours)

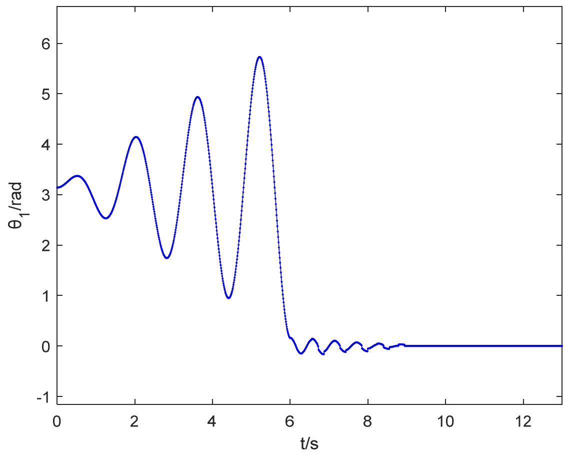


It can be clearly seen from the simulation curve that the ORRCF method combined with the PBC control scheme adopted in this paper makes the two swing angles converge to zero within 10s during the response time of the entire control process. At the same time, the two pendulum rods are stably maintained in the vertical upward position. The existing literature (Zhang et al., 2011) adopts a control method based on variable gain LQR, which makes the two pendulums converge to zero in 14 s. That is to say, the control scheme designed in this paper shortens the convergence time of the whole control process by 4s, and its control effect is better. Therefore, the control scheme designed in this paper has the characteristics of fast convergence speed and strong robustness for the inverted pendulum system.

**Figure 7** Response curve of pendulum 2 angle $\theta_2$ (see online version for colours)

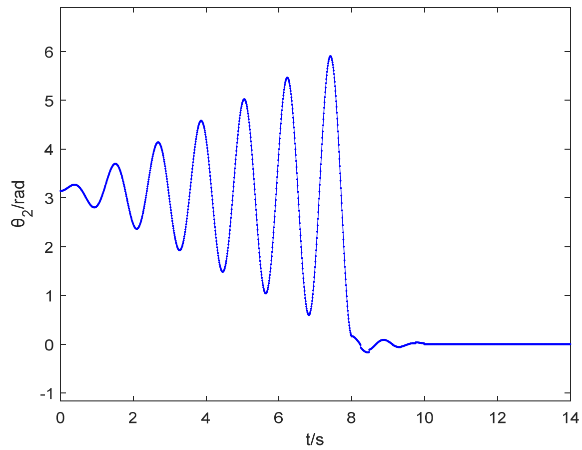


## 6 Conclusions

Aiming at the characteristics of multiple degrees of freedom, strong coupling and complex nonlinearity of the inverted pendulum system with limited guide rails, this paper combines the PBC method with the ORRCF method to design a control scheme, which improves passivity and robustness of the inverted pendulum system. It effectively overcomes the influence of external interference during the switching process of the swing control and the limited guide rail. The step-by-step start-up and steady-swing control of the double inverted pendulum system is realised. Moreover, the application of the PBC method is more practical in engineering design than the previous energy control methods, and has a certain value for the control of the actual inverted pendulum system.

## References

Åström, K.J. and Furuta, K. (2000) 'Swinging up a pendulum by energy control', *Automatica*, Vol. 36, No.2, pp.287–295.

Bi, S., Deng, M. and Xiao, Y. (2015) 'Robust stability and tracking for operator-based nonlinear uncertain systems', *IEEE Transactions on Automation Science and Engineering*, Vol. 12, No. 3, pp.1059–1066.

Bu, N. and Deng, M. (2011) 'Isomorphism-based robust right coprime factorization realization for nonlinear feedback systems', *Proceedings of the Institution of Mechanical Engineers, Part I: Journal of Systems and Control Engineering*, Vol. 225, No. 6, pp.760–769.

Bu, N. and Deng, M. (2016) 'Passivity-based tracking control for uncertain nonlinear feedback systems', *Journal of Robotics and Mechatronics*, Vol. 28, No. 6, pp.837–841.

Bu, N., Liu, H. and Li, W. (2021) 'Robust passive tracking control for an uncertain soft actuator using robust right coprime factorization', *International Journal of Robust and Nonlinear Control*, Vol.31, No. 14, pp.6810–6825.

Bu, N., Pang, J. and Deng, M. (2020) 'Robust fault tolerant tracking control for the multi-joint manipulator based on operator theory', *Journal of the Franklin Institute*, Vol. 357, No. 5, pp.2696–2714.

Chen, J. and Qian, D. (2021) 'Three controllers via 2nd-order sliding mode for leader-following formation control of multi-robot systems', *International Journal of Advanced Mechatronic Systems*, Vol. 9, No. 2, pp.85–101.

Deng, M. and Bu, N. (2012) 'Robust control for nonlinear systems using passivity-based robust right coprime factorization', *IEEE Transactions on Automatic Control*, Vol. 57, No. 10, pp.2599–2604.

Deng, M. and Bu, N. (2016) 'Passivity-based tracking control for uncertain nonlinear feedback systems', *Journal of Robotics and Mechatronics*, Vol. 28, No. 6, pp.837–841.

Deng, M., Bu, N. and Inoue, A. (2009) 'Output tracking of nonlinear feedback systems with perturbation based on robust right coprime factorization', *International Journal of Innovative Computing, Information and Control*, Vol. 5, No.10(B), pp.3359–3366.

Deng, M., Maekawa, T., Bu, N., et al. (2011) 'Actuator fault detection on a process control experimental system using combined observers', *Proceedings of the Institution of Mechanical Engineers, Part I: Journal of Systems and Control Engineering*, Vol. 225, No.6, pp.807–813.

Deng, M., Saijo, H. and Inoue, A. (2006) 'A robust real time method for estimating human multi-joint arm viscoelasticity', *International Journal of Innovative Computing, Information and Control*, Vol. 2, No. 4, pp.705–721.

He, C., Xu, X., Zhong, X. et al. (2021) 'PID parameters tuning of rotary inverted pendulum based on improved particle swarm optimization algorithm', *Techniques of Automation and Applications*, Vol. 40, No. 12, pp.10–15.

Henmi, T., Chujo, M., Ohta, Y., et al. (2014) 'Reproduction of swing-up and giant swing motion of Acrobot based on a technique of the horizontal bar gymnast', *Proceeding of the 11th World Congress on Intelligent Control and Automation*, pp.2613–2618.

Henmi, T., Deng, M., Inoue, A. et al. (2005) 'Swing-up control of a serial cart-type double inverted pendulum system', *Transactions of the Japan Society of Mechanical Engineers*, Vol. 71, No. 704, pp.1269–1275.

Henmi, T., Deng, M., Inoue, A., et al. (2003) 'Reverse order swing-up control of serial double inverted pendulums', *SICE 2003 Annual Conference*, Vol. 2, pp.1445–1450.

Henmi, T., Park, Y., Deng, M., et al. (2010) 'Stabilization controller for a cart-type inverted pendulum via a partial linearization method', *Proceedings of the 2010 International Conference on Modelling, Identification and Control*, pp.248–253.

Liu, X., Zhang, Q., Cheng, J. et al. (2021) 'Research on gait trajectory adaptive control method of bionic biped robot', *Computer Simulation*, Vol. 38, No. 3, pp.298–302.

Liu, X., Zhang, Q., Cheng, J. et al. (2021) 'Research on adaptive control method of gait trajectory of bionic biped robot', *Computer Simulation*, Vol. 38, No. 3, pp.298–302.

Takasu, K., Deng, M., Noge, Y. et al. (2020) 'Chattering and bias-free design of operator-based nonlinear sliding mode control for a WPT system', *International Journal of Advanced Mechatronic Systems*, Vol. 8, No. 4, pp.127–135.

Zhang, Y., Li, H., Miao, Z. et al. (2011) 'Swing-up of double inverted pendulum based on variable gain LQR technique', *System Engineering Theory and Practice*, Vol. 31, No. 7, pp.1341–1355.

Zhou, Y. (2020) 'Research on LQR control of circular inverted pendulum system improved genetic algorithm', *Mechanical Engineering and Automation*, Vol. 49, No. 3, pp.31–32.